CHARACTERIZING BEST METHODS FOR IMPROVING LIGHT YIELD IN CSI(TL) SCINTILLATORS

An Undergraduate Research Scholars Thesis

by

KENSINGTON N. VINCENT

Submitted to the LAUNCH: Undergraduate Research office at
Texas A&M University
in partial fulfillment of the requirements for the designation as an

UNDERGRADUATE RESEARCH SCHOLAR

Approved by
Faculty Research Advisor: Rupak Mahapatra, Ph.D.

May 2023

Major: Physics

RESEARCH COMPLIANCE CERTIFICATION

Research activities involving the use of human subjects, vertebrate animals, and/or biohazards must be reviewed and approved by the appropriate Texas A&M University regulatory research committee (i.e., IRB, IACUC, IBC) before the activity can commence. This requirement applies to activities conducted at Texas A&M and to activities conducted at non-Texas A&M facilities or institutions. In both cases, students are responsible for working with the relevant Texas A&M research compliance program to ensure and document that all Texas A&M compliance obligations are met before the study begins.

I, Kensington N. Vincent, certify that all research compliance requirements related to this Undergraduate Research Scholars thesis have been addressed with my Faculty Research Advisor prior to the collection of any data used in this final thesis submission.

This project did not require approval from the Texas A&M University Research Compliance & Biosafety office.

TABLE OF CONTENTS

Page

ABSTRACT

Characterizing Best Methods for Improving Light Yield in CsI(Tl) Scintillators

Kensington N. Vincent
Department of Physics and Astronomy
Texas A&M University

Faculty Research Advisor: Rupak Mahapatra, Ph.D.
Department of Physics and Astronomy
Texas A&M University

Due to excess gravitational force in the observable universe, it is estimated that 85% of the matter in the universe does not interact with electromagnetic, or light, waves. This matter has been dubbed "Dark Matter:", and the search for how to detect these particles has been the focus of many scientists for decades. One hypothesis is that dark matter is a WIMP (weakly interacting massive particle). These particles rarely interact with normal matter, so it is necessary to make extremely low-energy sensitive detectors to distinguish minute differences in closely residing energy peaks. One form of detection is through scintillators which take high energy electromagnetic waves (gamma rays) and through the intrinsic properties of the CsI(Tl) crystal transform them into visible light rays. These light rays are able to be detected through a photomultiplier tube (PMT). Once the gamma ray is transformed, the light ray must be reflected into the photocathode of the PMT which calls for a completely reflective material to be wrapped around the crystal to ensure that the highest percentage of transformed electromagnetic waves enter into the PMT to be detected, or in other words, a high light yield. To increase the ability of CsI(Tl) scintillator detectors to do so, a new wrapping material will be used on the innermost layer of the detector. The new wrapping material is a 3M^{TM} Enhanced Specular Reflector (ESR) material which is hypothesized

to produce a higher light yield with better resolution than the original wrapping of plumber's tape due to its high reflectivity. Two different types of measurements were carried out to test this hypothesis. First, a source of ^{60}Co was used to test the difference between the wrappings. The test was run an hour for the original and the new wrapping. We observe a 35% increase in the ADC count for each ^{60}Co energy peak and 15% decrease in the value of the standard deviation around those peaks. Secondly, a source of ^{241}Am was used to test the low-energy capabilities of the new material. Here also we see a significant increase in the ADC count for the two energy peaks of the ^{241}Am source. Due to the high photon reflectivity capability of the new ESR film, our detector is more capable of collecting photons created by even low-energy interactions. As we know Dark Matter produces very low-energy recoils, while interacting with the detector target material, so the ability to contain a maximum number of photons within the detector volume will help us move one step closer to finding the rare interaction. Because of this significant increase in light yield and general decrease in standard deviation, it is clear that the ESR material has a greater ability to gather higher resolution data than its predecessor. This could lead to a greater understanding of low-energy particles, which in turn could help us understand what Dark Matter really is.

DEDICATION

To my loving family and my wonderful fiancé, Hunter Boyer, for supporting me in my education and research endeavors.

ACKNOWLEDGMENTS

Contributors

I would like to thank my faculty advisor, Dr. Mahapatra, and my graduate student mentor, Shubham Verma, for their guidance and support throughout the course of this research. I would also like to thank Ishita Poddar, Samikshya Mahapatra, and Mark Platt for their contribution to the experimental design. Special thanks to Sharada Sahoo for guidance in data analysis.

Thanks also go to my friends and colleagues and the department faculty and staff for making my time at Texas A&M University a great experience.

All other work conducted for the thesis was completed by the student independently.

Funding Sources

Undergraduate research was supported by the Presidential Impact Fellowship provided by Texas A&M University. Support was also given by the Los Alamos National Lab and the National Laboratories Office at Texas A&M University.

NOMENCLATURE

CsI(Tl)	Cesium-Iodide (Thallium)
^{60}Co	Cobalt 60
^{241}Am	Americium 241
PMT	Photomultiplier Tube
ESR	Enhanced Specular Reflector
PET	polyethylene tereohthalate
A	Amps
V	Volts
eV	Electron Volts
ADC	Analog to Digital Converter
s	Seconds
WIMP	Weakly Interacting Massive Particle
ALP	Axion-like Particles

1. INTRODUCTION

Increasing the light yield and resolution of gamma ray detectors for low energy and close energy peaks will have immense applications in the areas of particle and astrophysics, especially in the search for Dark Matter. In the past century, astronomers have observed in galaxies a significant amount of mass that appeared to be “missing” in relation to the amount of gravitational force needed to keep the stars from escaping from the galaxy’s gravitational pull.

The most well known pioneering observation of this was by Fritz Zwick in 1933; he observed that the velocities of galaxies in the Coma cluster were much higher than the expectation value calculated by the sum of the individual galaxy masses [1]. Later “observations in the 1970s of the motion of gas and stars in the outskirts of galaxies” confirmed that there must be some sort of “missing mass” [1]. This mass was observed by gravitational lensing to be generally located in large halos of galaxies and clusters of galaxies [1]. Over the next decades, accumulated data “showed that the total amount of matter in the universe is approximately five times greater than the amount of baryonic matter”, or matter that is composed of protons and neutrons [1].This baryonic matter is normal matter that is composed of quarks and interacts with the four fundamental forces, including electromagnetic waves.

Dark Matter, the name itself suggests that it doesn’t normally interact via electromagnetic (EM) interaction and hence are "dark". There are a few hypotheses as to what constitutes this Dark Matter. One hypothesis is that some do interact electromagnetically but with very less interaction probability than normal "light" matter such as axion like particles (ALP). Another is that Dark Matter interacts via weak interaction such as weakly interacting massive particles (WIMP). WIMPs are neutral, highly massive particles that interact only through gravitational and weak nuclear forces which would make them invisible to the typical forms of electromagnetic wave detection.

These two are the primary candidates for Dark Matter and both interact with a very low scattering cross-section. That means they rarely interact with ordinary matter and if they interact

they impart very low energy to the target material. For example a 10-1000 GeV WIMP will produce only 1-100 keV recoil energy after an interaction [2]. Thus, it is imperative to develop detectors with the ability to detect low-energy particles through a low threshold and distinguish minute differences in closely residing energy peaks through a good energy resolution. This better energy resolution would also allow the hypothesized Dark Matter to be distinguished from background noise such as cosmic rays (i.e. muons) or inherent electrical noise. In order to develop these detectors, smaller, simpler detectors will first be used with known radioactive sources of low-energy to determine how well the components of the detector can make these precise measurements.

The use of scintillators "remains one of the most useful methods available for the detection and spectroscopy of a wide assortment of radiations"[3], and especially cesium iodide crystals laced with thallium (Cs(Tl)) because of its "high light output, good energy resolution and large absorption coefficient to high energy particles" [4]. Cs(Tl) also is "resistant to thermal and mechanical shock" [5] which makes it a reliable crystal to use. Though much research has been done with "CsI(Tl) scintillators for a wide variety of X Ray imaging applications" [6], there is more to be learned about its ability to detect gamma rays. There is also much that can be done to enhance the light yield of gamma rays through not only the crystal itself, but especially through the wrapping material.

Through the inherent properties of the scintillator crystal, gamma rays are transformed into electromagnetic waves in the visible light spectrum. Once the light is in the visible light spectrum, in order to detect it, it must be reflected as efficiently as possible into the photomultiplier tube (PMT) to be detected and measured. This requires the crystal to be wrapped tightly in a material that will allow gamma rays to pass through, but completely reflect visible light. In my research a 3M^{TM} non-metallic polymer film will be used, as its normal reflectance is stated to be "greater than 98.5%" [7] which is a significant increase from the most typical form of wrapping, plumber's tape.

To understand how much greater the resolution of individual peaks of gamma ray spectroscopy can be with improved wrapping materials, experiments will be performed and compared against the most typical form of the innermost wrapping around a CsI(Tl) scintillator, plumber's

tape. Because of the high reflectivity of the 3M^{TM} material, the new wrapping of a CsI(Tl) crystal is expected to produce a significantly higher light yield and a better resolution of especially low energy and closely residing energy peaks in the two known sources of ^{60}Co and ^{241}Am that were tested.

2. MATERIALS AND METHODS

2.1 Experimental Setup

The most fundamental component in the experiment is the CsI(Tl) scintillator crystal. We use CsI(Tl) scintillators because they are performant in areas such as light emission emitting 54,000 photons/MeV (45% of NaI(Tl)) and a high density of 4.51 g/cm^3 creating a high chance of interacting with an external particle [8]. Additionally, CsI(Tl) scintillators can be used for particle discrimination using pulse shape analysis since it has two different decay times of 0.6 μs and 3.5 μs having two different decay processes. Light intensity from these decay processes vary depending on types of particle interaction, hence particle discrimination can be done from the shape of the pulse [4]. Lastly, the thallium (Tl) atoms work as crucial activators allowing the scintillator to convert high energy gamma rays to visible light rays with a wavelength of 540 nm [6]. Additionally, in comparison to other inorganic Alkali-Halide scintillators, CsI(Tl) shows a larger gamma-ray absorption coefficient per unit size and lower hygroscopicity. [3].

Scintillators "convert the kinetic energy of charged particles" (in this case gamma rays) "into detectable light" [3]. The crystal is the ionic compound of cesium and iodide, but is doped with thallium. This dopant, or activator, gives the crystal its intrinsic transformative ability. When a gamma-ray passes through the detection medium, it excites the valence band electrons to the conduction band which creates a positive hole in the valence band. If there was no dopant, the electron would quickly deexcite to the valence band, releasing a gamma-ray of the same energy level as the incident ray. This is because the electron can only release light waves in certain levels of energy. Any levels of energy between those quantized states are in what is referred to as the forbidden gap.

However, the energy levels of the valence and conduction bands of the activator reside within that forbidden energy gap. Because of this, once the electron is excited to the conduction band of the crystal, the positive hole created by the elevated electron will quickly drift to the valence band of the activator due to its ionization energy being lower than that of the cesium

iodide. The electron in the valence band will then drift until it encounters an ionized activator. It will then drop into the activator site to create a neutral configuration. Lastly, the electron will deexcite to the ground state of the activator. This deactivation will cause a photon to be ejected in the visible light rays. Once the light is in the visible spectrum, in order to detect it, it must be reflected as efficiently as possible into the photomultiplier tube (PMT) to be detected and measured. This requires the crystal to be wrapped in a material that will allow gamma rays to pass through, but completely reflect visible light.

The experimental setup utilized a CsI(Tl) crystal which was 2" x 2" x 12" in dimension which was cut in half and polished on the cut ends resulting in two nearly identical 6" crystals. The crystals were cut in half to have a larger light collection efficiency and decrease the contribution of electronic noise [9].The crystal was inspected to ensure there were minimal scratches, cracks and discoloration due to its hygroscopic nature. The sides were then carefully cleaned, handled, and stored to avoid any smudges or other impurities that could result in unwanted refraction of light rays. This is shown in Figure 1 (a).

(a) Unwrapped 6 inch CsI(Tl) crystal. The crystal is very clear, free from impurities, and major chips or scratches.

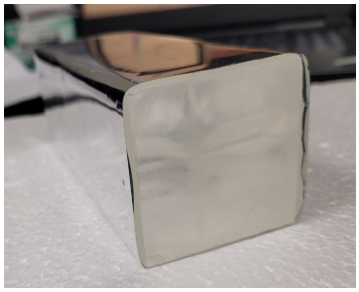

(b) Crystal wrapped with 3M™ ESR material. The open end is where the crystal will connect to the PMT photocathode

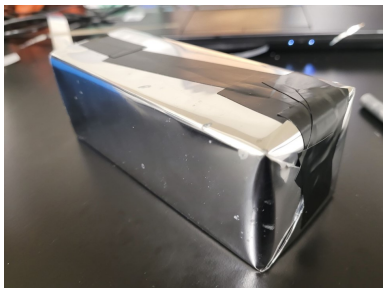

(c) Closed end of the 3M™ ESR material wrapped crystal. It is secured with black electrical tape to keep the material tight against the crystal.

Figure 1: CsI(Tl) crystal with the first layer of 3M™ ESR wrapping.

One crystal was first wrapped in white plumbing tape, which has been used on previous experiments with CsI(Tl) scintillators. Since the goal of the wrapping is to reflect all visible light

back into the crystal and eventually into the photocathode of the PMT, the white color of the tape would be ideal for this. The tape also clings easily to the crystal so that any air pockets or folds were easily smoothed out with a ruler or finger. However, when stretched the tape can become translucent, which creates a need for multiple layers to ensure there is a consistent white wrapping around the crystal.

The other crystal was wrapped in 3M^{TM} Enhanced Specular Reflector (ESR) material, "an ultra-high reflectivity, mirror-like optical enhancement film" that is made of a "multi-layer polymer". It is stated to have a "nominal reflectance greater than 98.5%" [7] across the visible spectrum. The wrapping of the material around the crystal was difficult, as great care was taken to avoid any air bubbles, folds, or space between the crystal and wrapping material that could result in unwanted refraction of visible light rays. The most difficulty in folding was at the closed end, shown in Figure 1 (c). A 2" x 2" piece of material was set on the closed side while a larger piece was wrapped around the four long sides and the excess was folded over the closed end of the crystal to keep the small 2" x 2" piece of material tight against the crystal. It was then all secured with black electrical tape. The result was airtight and since the material is opaque, it only needed one layer. The final wrapping of this first layer is shown in Figure 1 (b) and (c).

On both crystals a second layer of an aluminized PET (polyethylene terephthalate) material was then put over the inner layer of plumber's tape or ESR material. This reflective material was wrapped around each crystal similar to the ESR material. This was done in an effort to reflect incoming background noise away from the crystal. This is shown in Figure 2 (a). Lastly each crystal was wrapped in black electrical tape. This tape held the previous two layers tightly to the crystal. It also provided another layer to protect against any light leaks coming in as background noise.

Once the crystals were wrapped they were then attached to the photocathode of a PMT specific to the visible light wavelength range using silicone optical coupling grease. This is shown in Figure 2 (b). Once a secure attachment was made, a thin sheet of aluminized PET was wrapped around the connection point which was wrapped tightly with black electrical tape to prevent any

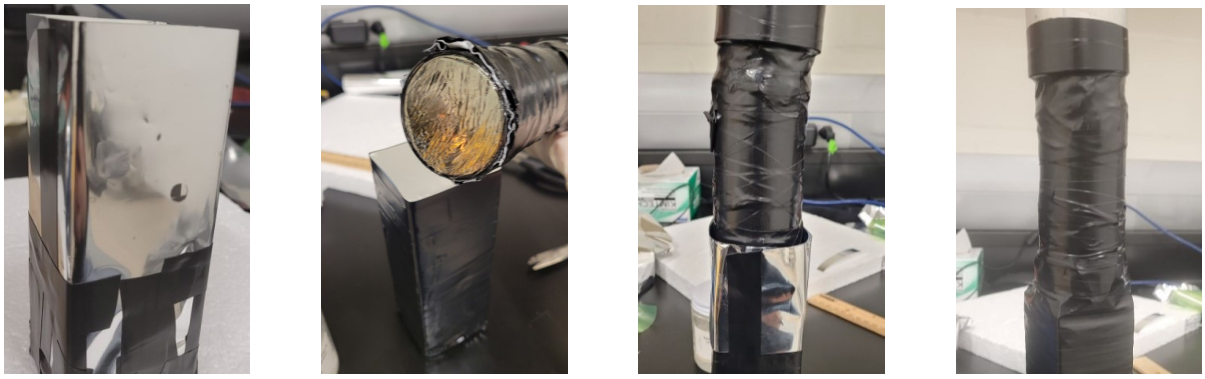

(a) Scintillator crystal wrapped with Aluminized PET material after the first layer of reflective material. This PET material was to reflect background light noise away from the scintillator.

(b) Photocathode of PMT coated with optical coupling grease which will be attached to the open side of the fully wrapped crystal.

(c) Aluminized PET material around the connection point between the PMT photocathode and the crystal to prevent background noise coming in at the connection point.

(d) Black electrical tape wrapped around the connection point to prevent light leakage and background noise.

Figure 2: Scintillator detector assembly process from 2nd layer to fully wrapped.

light leaks and secure the PET material. This process is shown in Figure 2 (c) and (d). A complete diagram of this setup is shown in Figure 3.

The photocathode of the PMT works as a consequence of the photoelectric effect. Once the incoming high level photon is transformed in the scintillator crystal into a photon with energy within the visible light spectrum, with ideal complete internal reflectance, it will reflect off the first layer of wrapping material until it reflects into the photocathode of the PMT. Once the photon hits the photocathode, an electron of proportional energy will be ejected on the opposite side of the photocathode into the PMT. This is due to the photoelectric effect which describes the phenomenon that happens when an electron is ejected from a material when electromagnetic radiation of sufficient energy hits it. This sufficient energy is called the work function, and any remaining energy from the photon is then transferred to the electron as kinetic energy. This means that each photoelectron will have a kinetic energy proportional to the energy of the incoming photon, and if the kinetic energy of the electron can be measured then the energy of the incident photon can be measured.

Once the electron is ejected, it then goes through a focusing electrode to the electron multiplier. The electron multiplier consists of a collection of dynodes which are held at increasingly

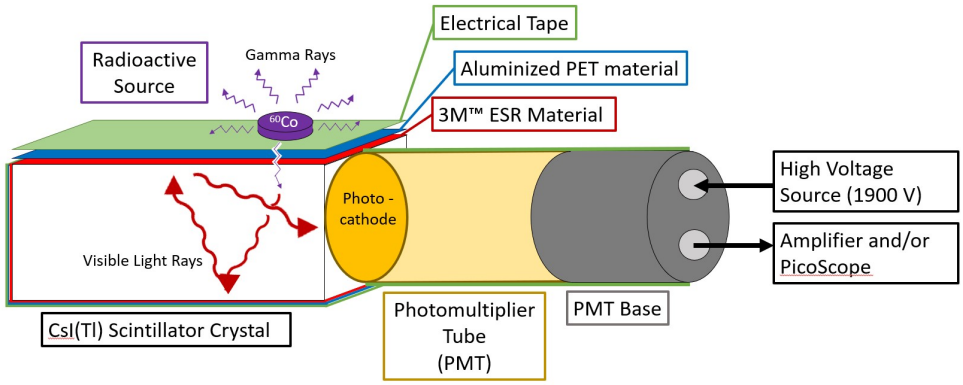

Figure 3: Scintillator Detector Diagram displaying the different layers of wrapping material, an example of a radioactive source, the scintillation process, PMT (with its photocathode), and base.

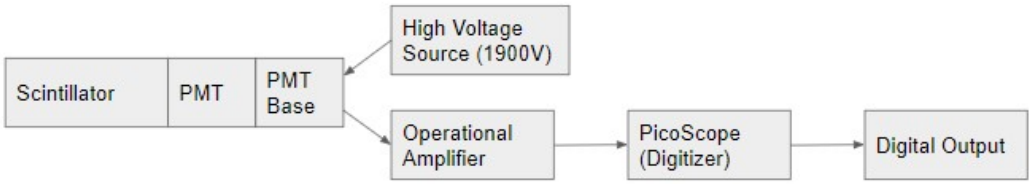

Figure 4: Circuitry flowchart diagram of detection hardware.

positive potentials. Due to the internal electric field the electron moves to the first dynode and once it hits the dynode a group of low energy electrons are emitted which then move towards the second dynode. This continues through all the dynodes with the number of emitted low energy electrons at each dynode increasing until this group of electrons hits the anode. The electrons hitting the anode produce a sharp current pulse that is easily detectable to our set-up. This analog signal goes through the PMT holder and to the digitizer, the PicoScope, which converts that analog signal into a digital signal which we can see on the PicoScope software.

The PMT was attached to a base which allowed it to be connected to a high voltage source of 1900 V which operated at 800-870 µA. With the experiments using ^{241}Am an operational amplifier

was used to allow the digitizer to analyze the low-energy peaks of ^{241}Am. Otherwise the PMT base was connected directly to the digitizer. In the case of ^{241}Am, this operational amplifier was then connected to the digitizer, the PicoScope 5442D MSO, which was then connected to a computer with the PicoScope software. The only part of the apparatus that was changed for each experiment was the scintillator crystal itself and whether or not the operational amplifier was used; the PMT and PMT base were the same in every experiment. This entire set up is shown in the diagram of Figure 4 and a photo is found in Figure 5.

Each test was performed in the same physical space. The scintillator detector (crystal, PMT, PMT base) was placed into a lead brick structure which enclosed the detector with 6 inches of lead on every side of it with exception of the small opening where the wires were placed as shown in Figure 5. This not only eliminated light noise, but greatly reduced the background noise due to cosmic rays and other high energy waves. Each test was also performed with the lights in the lab turned off to further protect against high levels of background noise.

(a) Front of the lead structure displaying the small, necessary opening where the wires can come out to connect to the rest of the hardware. The scintillator detector is placed completely in this lead structure.

(b) Full view of the lead structure from behind. Each wall on the lead structure, except for the small opening for the wires, is 6 inches thick. This is to reduce high energy background noise like cosmic rays.

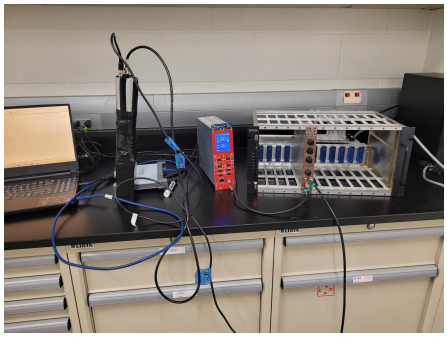

(c) Full display of all hardware and software. These are, from left to right: computer with PicoScope software, scintillator detector, PicoScope digitizer, high voltage source, operational amplifier. The only difference in actual setup is that the detector would be inside the lead structure.

Figure 5: Full setup of experimental hardware and software.

The first tests were run using a source of 1 μCi of ^{60}Co. ^{60}Co has a half life of a little over 5 years and undergoes beta decay to ^{60}Ni and emits two closely residing gamma rays of energies

1.17 MeV and 1.33MeV. A huge advantage of using ^{60}Co is its longer half-life for its high intensity emissions of gamma-rays. However, the most important attribute of ^{60}Co for our experiment is its dual high intensity gamma peaks. The purpose of these tests were to demonstrate a greater light efficiency and therefore greater resolution when the ESR material was used. This would be evident in the resolution between the 1.17 MeV and 1.33 MeV gamma peaks found in ^{60}Co. If the new ESR material is able to more clearly resolve the two closely residing gamma peaks in comparison to the previous wrapping material, it can be concluded that the ESR material would be better suited for other experiments.

The small disk containing the sample of ^{60}Co was taped onto the crystal near the connection point to the PMT as shown in Figure 3. This was done in an effort to increase light efficiency as the light would have to travel less to reach the photocathode of the PMT. The detector was then placed horizontally into the lead structure and closed off with a lead brick.

The first test of ^{60}Co was run with the original wrapping of the plumber's tape. This test was run for an hour with a trigger threshold of -15 mV which resulted in 70,000 recorded events. This was set using the PicoScope software which was able to record energy levels between +500 mV and -500 mV. The second test of ^{60}Co was run with the crystal wrapped in the ESR material. This test was run with the same trigger threshold of -15 mV for an hour with a range of ±500 mV; however, 80,000 events were recorded during that time. The ESR material had another 10,000 triggered events in the 1 hour test duration more than the original wrapping. This is because the ADC count, or light yield, increased with the better wrapping, and the signals which were not able to cross the energy threshold previously now are able to. This allowed the detector to pick up more low-energy events that were rejected in previous tests. These tests are shown in Figures 9, 10, and 11.

The second set of tests were run using a source of ^{241}Am. The main products of the radioactive decay of ^{241}Am are ^{237}Np, an alpha particle, and a very weak gamma ray byproduct. Since the focus of the experiment was not on the alpha decay of ^{241}Am but rather the gamma ray emission, the sample of ^{241}Am was wrapped in paper to prevent the alpha particle emissions from disturbing

the experiment. The main advantage in using ^{241}Am comes from the weak gamma ray emission. This weak gamma ray emission will allow the true extent of the reflectivity of the ESR material to be revealed.

The goal of this set of experiments was to demonstrate the better ability of the ESR material to show low-energy peaks with higher resolution as compared to the original wrapping. Since ^{241}Am emits low energy gammas between 0.013-0.026 MeV and also one of 0.06 MeV, an operational amplifier was used to amplify this low energy signal. The gain of the operational amplifier was set to 20x and both tests were run for 3 hours.

In the first test with the original wrapping the trigger threshold was set to -30 mV with a range of ±1 V. This first test recorded 200,000 events. The second test was run with the new ESR wrapping which had a trigger threshold of -45 mV and a range of ±1 V. 180,000 events were recorded in this test, and although this is less than the original wrapping it is to be expected with a trigger threshold that is 50% higher than the original wrapping. These tests are shown in Figures 12, 13, and 14.

2.2 Data Processing and Error Elimination

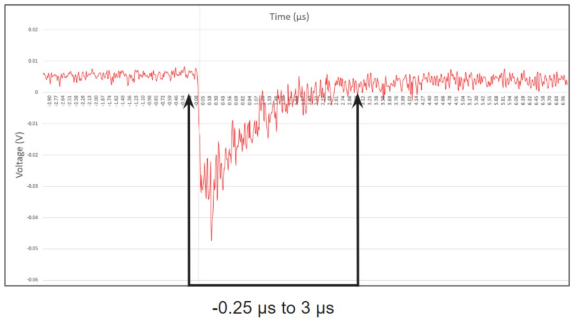

(a) A plot of each saved energy point during a captured event. The y-axis is shown in volts and the x-axis is in microseconds. The screenshot shows a range of 10 µs with the event occurring at 3 µs from the left. The range of the data analyzed was taken from 0.25 µs before the event to 3 µs after.

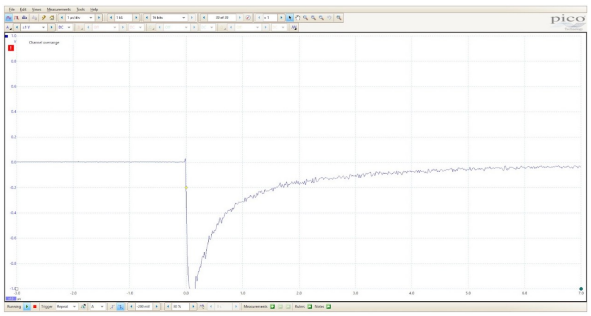

(b) A screenshot of the PicoScope software during an overrange event. An overrange message is displayed in the top left corner of the graph. This overrange event is shown by the most negative part of the peak goes off past the end of the screen where the range is set.

Figure 6: Display of Picoscope software during a captured event.

With each individual event the PicoScope would record 1,000 values in a 10 µs window, 3

μs before the trigger was hit and 7 μs afterwards. Each event would last approximately 3 μs. These 1000 values were recorded in a .csv file with their associated times in relation to the trigger event. Each .csv file would then be run through a python code which would take the integral under the curve of the trigger event from 0.25 μs before the event to 3 μs after as shown in Figure 6. The integral of each curve was then compiled into a list from which a histogram was generated which showed the differing energy peaks.

Table 1: ^{60}Co Original Wrapping Systematic Check (a.u.)

Set of 10,000	**Peak 1: Mean**	**Standard Deviation**	**Peak 2: Mean**	**Standard Deviation**
1	19.86±0.16	2.193±0.15	22.84±0.15	2.239±0.21
2	19.88±0.17	2.050±0.21	22.51±0.32	2.545±0.36
3	20.08±0.15	2.326±0.19	22.65±0.22	2.299±0.25
4	19.82±0.087	2.225±0.12	22.81±0.14	2.214±0.17
5	19.73±0.083	2.261±0.13	22.67±0.12	2.038±0.14
6	19.84±0.089	2.406±0.13	22.67±0.15	2.090±0.16
7	19.78±0.094	2.248±0.14	22.91±0.086	1.915±0.11

Table 2: ^{60}Co New Wrapping Systematic Check (a.u.)

Set of 10,000	**Peak 1: Mean**	**Standard Deviation**	**Peak 2: Mean**	**Standard Deviation**
1	28.61±0.067	1.717±0.090	33.27±0.065	1.803±0.094
2	27.92±0.059	1.651±0.080	32.63±0.075	1.540±0.088
3	27.69±0.074	1.801±0.010	32.08±0.089	1.807±0.010
4	27.50±0.052	1.654±0.067	31.98±0.11	1.650±0.12
5	27.29±0.047	1.673±0.065	31.70± 0.11	1.757±0.16
6	27.02±0.058	1.565±0.075	31.73±0.078	1.580±0.11
7	26.99±0.059	1.59±0.077	31.51±0.073	1.743±0.10
8	26.99±0.050	1.717±0.070	31.49±0.079	1.663±0.10

There were two main limitations in working with the PicoScope, a limited range of energy levels could be recorded in relation to the set trigger threshold and only 10,000 events can be recorded at a time before it saves the data. The PicoScope could only record energy values that

were less than the set range. If the energy peak was greater than the set range, a channel overrange warning appeared, as shown in Figure 6. In the .csv file for that event, each one of the 1,000 data points that was over-range would have an error message instead of an energy value. This was remedied by replacing each of those values with the greatest value limit of the range. Though this method would result in slightly lower values for each integral taken, the tests rarely went over-range. The range could not be increased because if the range is too large in comparison to the trigger threshold value, the PicoScope will not register events. Because of this, each range was set at the largest possible value while still being able to detect events for the set threshold. The second limitation was the PicoScope needing to stop registering events and save the files every 10,000 events. Saving the files took around 2-3 minutes each time, so the 3 hour tests weren't truly 3 hours of continuous recording. It was 3 hours of combined saving breaks and recording.

Because of the long run time of the experiments, a systemic check was run to ensure that comparable data was received at the beginning of the test and the end and there was no drifting due to excess heat or other complications as the tests could be multiple hours long. The total light yield of CsI(Tl) scintillator crystals is dependent on temperature [10]. Because of this, if any part of the detector were to produce sufficient heat due to running for too long, the overall light yield and resolution could be negatively affected. This was done by splitting the ^{60}Co 1 hour tests into 10,000 event sections (which is about every 8.5 minutes) and comparing the statistics for each separate section. This was done for both the original wrapping and the new ESR wrapping. The mean and standard deviation with their respective uncertainties are shown in Tables 1 and 2 for each peak. Through looking at each test in Figures 7 and 8, the variations in mean and standard deviation are within their respective uncertainties. Therefore, drifting due to overheating was eliminated as a significant possibility of error in our experiment.

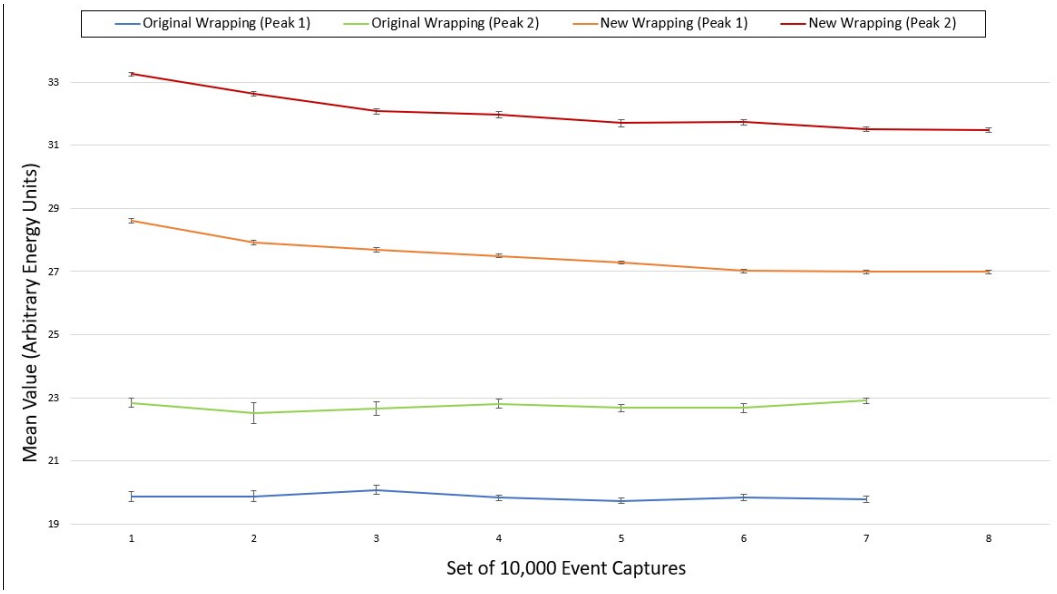

Figure 7: ^{60} Co systemic check for drifting over time. Plot of the mean with uncertainty in arbitrary energy units of each set of 10,000 events for both peaks for the original (shown in blue and green) and new ESR wrapping (shown in orange and red).

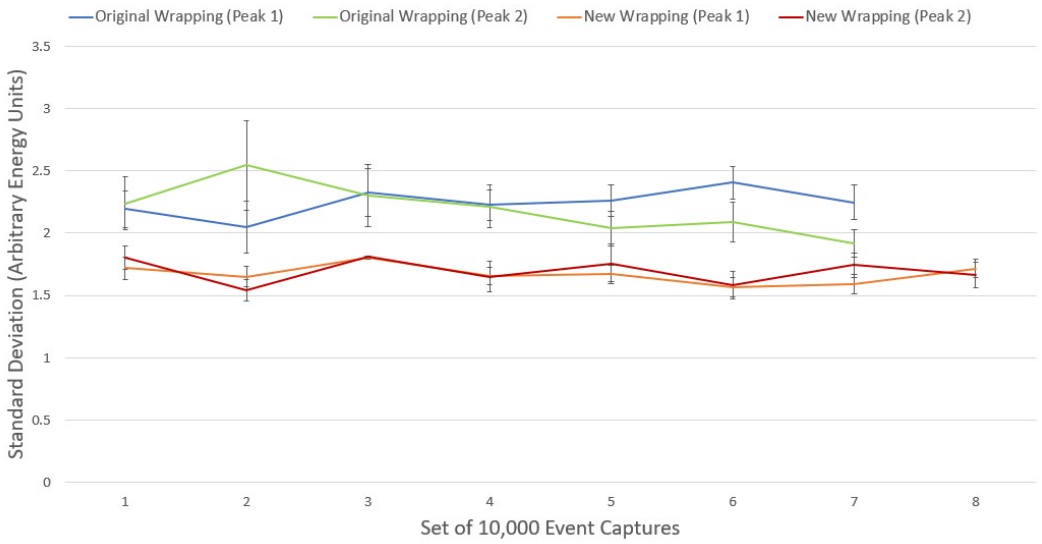

Figure 8: ^{60} Co systemic check for drifting over time. Plot of the standard deviation with uncertainty in arbitrary energy units of each set of 10,000 events for both peaks for the original (shown in blue and green) and new ESR wrapping (shown in orange and red).

3. RESULTS AND ANALYSIS

3.1 ^{60} Co Results

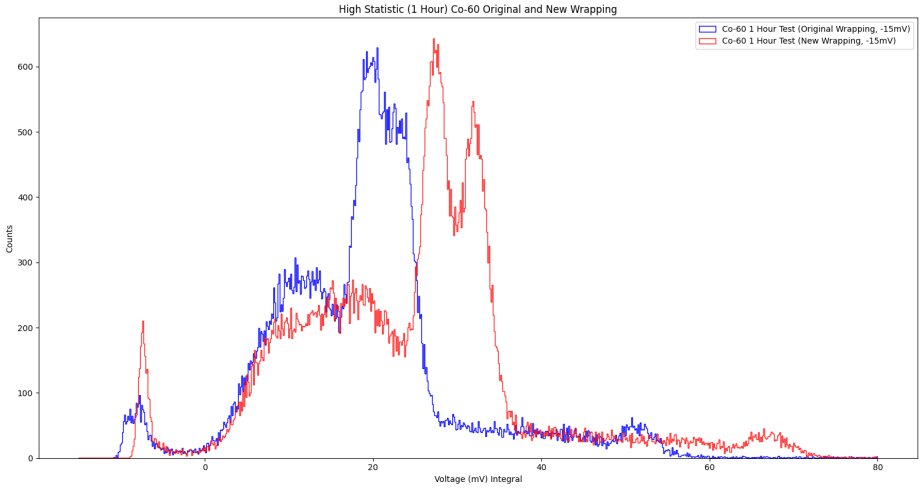

Figure 9: ^{60}Co 1 Hour Histogram Comparison Graph with the original wrapping test histogram shown in blue and the new ESR wrapping test shown in red. An increase of over 35% in the mean of each of the peaks is shown. The x-axis is displayed in arbitrary energy units.

The objective of the ^{60}Co tests was to compare the resolution between the 1.17 MeV and 1.33 MeV peaks for the original and new wrapping. This resolution was calculated by dividing the standard deviation of each peak by the mean. The resolution is dimensionless which is expressed as a percentage. A lower resolution percentage is better because the detector will be better able to "distinguish between two radiations whose energies lie near each other" [3]. If a better resolution is found in these tests using the ESR material, it would prove that the ESR material would be more advantageous in resolving WIMP from other background noise. This comparison is shown in Figure 9.

As shown in Figure 10, the two peaks, though distinguishable, appear close together in the plot of the original wrapping. The mean of the 1.17 MeV peak appears in the measured energy

Table 3: ^{60}Co Statistics (a.u.)

Wrapping	Peak	Mean	Standard Deviation	Resolution	Calibration Factor
$Original$	1	19.89	2.277	0.11	59.97
$Original$	2	22.73	2.172	0.10	58.60
New	1	27.43	1.739	0.06	42.76
New	2	32.01	1.814	0.06	41.61

units at 19.89 with a standard deviation of 2.277 which gives it a resolution of 11%. The 1.33 MeV peak had a similar resolution of 10% with its mean at 22.73 and its standard deviation at 2.172. The calibration factor from the measured energy units to known values of 1.17 MeV and 1.33 MeV is about 59.

The new ESR wrapping, shown in Figure 11, gave us a much higher light yield as shown in the higher mean values and lower calibration factor. The 1.17 MeV peak resided at 27.43 with a standard deviation of 1.739 which is a 37% increase in the mean as compared to the original wrapping, but a 23% decrease in the standard deviation. A similar result was found in the 1.33 MeV peak with a mean of 32.01 and a standard deviation of 1.814. This is a 40% increase in the mean and a 16% decrease in the standard deviation. The resolution for both peaks was 6% and the calibration factor was approximately 42.

The dramatic right shift of the mean and decrease in the standard deviation is evident in Figure 9 where the original wrapping plot is shown in blue and the new wrapping is shown in red. The increase in the mean, and the decreased calibration factor show that there is less light leakage, therefore greater internal reflection, in the new wrapping. This greater light yield also resulted in the low standard deviation and improved resolution with the new wrapping.

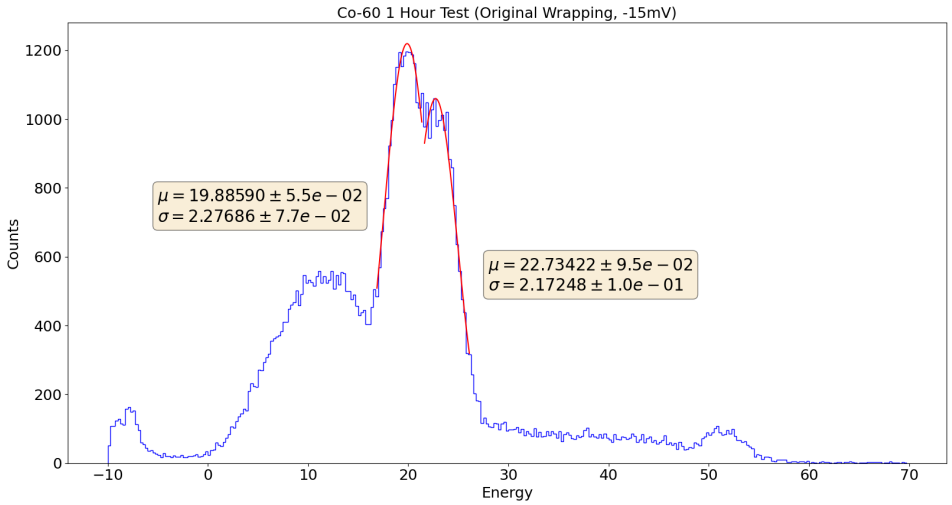

Figure 10: ^{60}Co 1 hour test histogram with original plumber's tape wrapping with a Gaussian fit displaying the mean and standard deviation of each peak. The first peak has a mean of 19.89±0.055 and standard deviation of 2.277±0.077 in arbitrary energy units. The second peak has a mean of 22.73±0.095 and a standard deviation of 2.172±0.10 in arbitrary energy units.

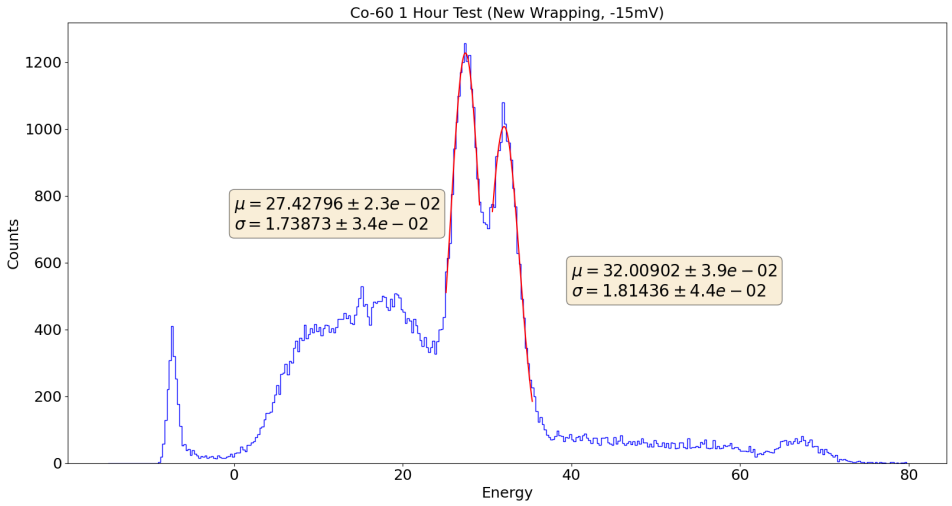

Figure 11: ^{60}Co 1 hour test histogram with new ESR wrapping with a Gaussian fit displaying the mean and standard deviation of each peak. The first peak has a mean of 27.43±0.023 and standard deviation of 1.739±0.034 in arbitrary energy units. The second peak has a mean of 32.01±0.039 and a standard deviation of 1.814±0.044 in arbitrary energy units.

3.2 ^{241}Am Results

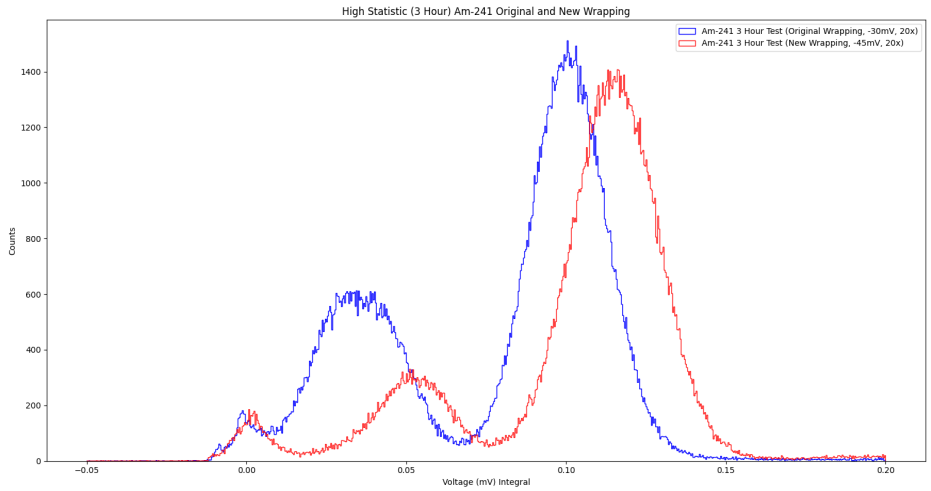

Figure 12: ^{241}Am 3 Hour Histogram Comparison Graph with the original wrapping test histogram shown in blue and the new ESR wrapping test shown in red. An increase of 14% in the mean of the 0.06 MeV peak is shown. The x-axis is displayed in arbitrary energy units.

The objectives of the ^{241}Am tests were to compare the resolution and light yield for low-energy peaks between the original and new ESR wrapping. Since WIMP's interact so rarely and weakly with normal matter, any interactions they do have will be very low energy. Because of this, it is important that the detectors are extremely sensitive at lower levels of energy. If the ESR material significantly improves the light yield for the low-energy peaks of ^{241}Am, it can be concluded that it will perform similarly for other low energy events.

As shown in Figure 13, two peaks from the ^{241}Am spectrum are found from the original wrapping test. The 0.06 MeV is shown furthest to the right with a mean of 0.1008 in the measured energy values and a standard deviation of 0.01198 which gives a resolution of 12%. ^{241}Am has 4 other known energy peaks ranging from 0.0139 to 0.0264 MeV which are assumed to be found in the leftmost peak which has a mean of 0.03515 and a standard deviation of 0.01475 which gives a resolution of 42%. The calibration factor, found using the 0.06 MeV peak, is approximately 591.

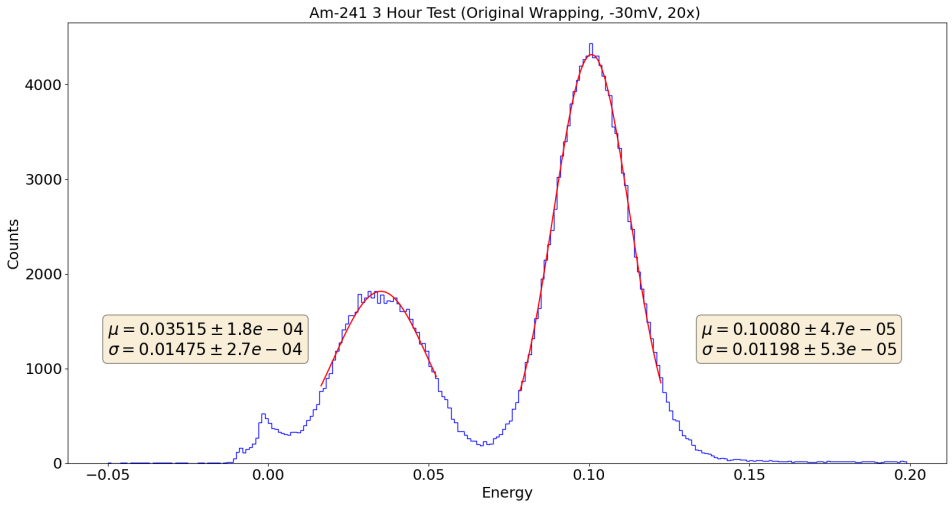

Figure 13: ^{241}Am 3 hour test histogram with original plumber's tape wrapping with a Gaussian fit displaying the mean and standard deviation of each peak. The first peak has a mean of 0.03515±0.00018 and standard deviation of 0.01475±0.00027 in arbitrary energy units. The second peak has a mean of 0.1008±0.000047 and a standard deviation of 0.01198±0.000053 in arbitrary energy units.

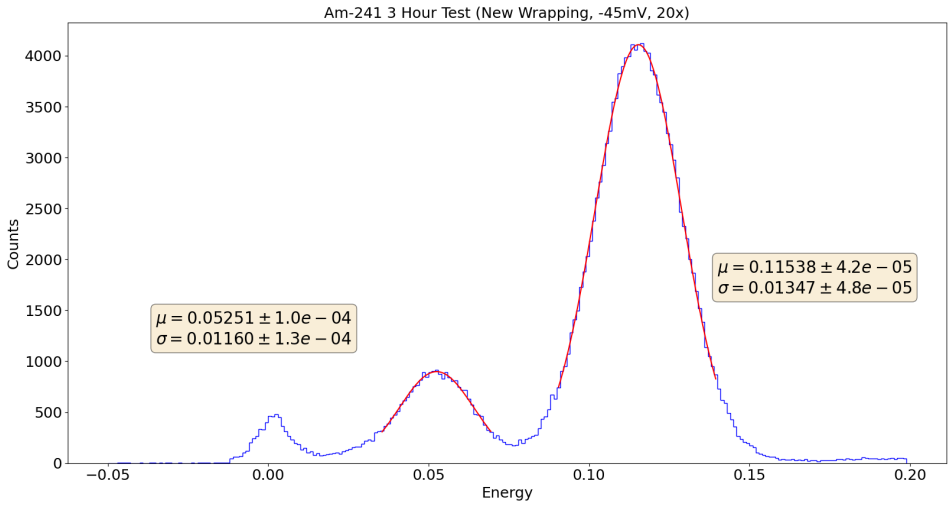

Figure 14: ^{241}Am 3 hour test histogram with new ESR wrapping with a Gaussian fit displaying the mean and standard deviation of each peak. The first peak has a mean of 0.05251±0.0001 and standard deviation of 0.01160±0.00013 in arbitrary energy units. The second peak has a mean of 0.1154±0.000042 and a standard deviation of 0.01347±0.000048 in arbitrary energy units.

The new ESR wrapping test, as shown in Figure 14, shows the same two peaks of ^{241}Am, 0.06 MeV and a grouping of the lower energy ones ranging from 0.0139 to 0.0264 MeV. The mean of the 0.06 MeV peak has the measured energy units of 0.1153 with a standard deviation of 0.01347 which results in a resolution of 12%. The mean of the range of lower peaks was found to be 0.05251 with a standard deviation of 0.01160 which results in a resolution of 22%. The calibration factor, found using the 0.06 MeV peak, is approximately 517.

The rightward shift of the mean energy peaks is shown in Figure 12. The new ESR wrapping (shown in red) resulted in a 50% increase in the mean, 21% decrease in the standard deviation, and 48% better resolution for the first peak compared to the original wrapping (shown in blue). For the 0.06 MeV peak, an increase of 14% in the mean, an increase of 12% in the standard deviation, and a similar resolution was observed. The calibration factor decreased by 13%.

Though the standard deviation was not decreased in the 0.06 MeV energy peak in the new ESR wrapping, the increase in the mean was still greater. As shown in Figure 12 the leftmost peak in the new graph is smaller than the original graph. The range of lower peaks 50% increase in mean as compared to the 14% increase in mean of the 0.06 MeV seemingly gives a mismatch of calibration. Using the calibration factor of 516.8, derived from the 0.06 MeV peak, the range of lower peaks gives us a mean of about 0.0269 MeV. This is much higher than the mean of the lower peaks in the original wrapping test which is about 0.02 MeV. However, due to the high threshold and the subsequent omission of those lower energy events, most of the leftmost part of that curve was cut off. If the threshold was set to a slightly lower energy, perhaps the entire curve of the lower peaks would have been visible. However, that would have compromised the resolution of the 0.06 MeV peak which was the goal of this experiment.

Table 4: ^{241}Am Statistics (a.u.)

Wrapping	**Peak**	**Mean**	**Standard Deviation**	**Resolution**	**Calibration Factor**
$Original$	1	0.03515	0.01475	0.42	591.3
$Original$	2	0.1008	0.01198	0.12	591.3
New	1	0.05251	0.01160	0.22	516.8
New	2	0.1153	0.01347	0.12	516.8

4. CONCLUSION

4.1 Conclusion

In the search for Dark Matter, the most probable hypothesis is that they are WIMPs, weakly interacting massive particles. These particles only interact through gravitational and weak nuclear forces which would make them invisible to the common forms of electromagnetic detection. WIMPs have a very low scattering cross-section which means when the interact with normal matter, they impart very low energy to the material. Because of this, it is of paramount importance to develop detectors with the ability to detect low-energy particle interactions. This would require the detector to have a high light yield and good resolution at low energies.

It was successfully shown that the 3M™ ESR material significantly increased the light yield in CsI(Tl) scintillators through the two experiments done with ^{60}Co and ^{241}Am sources. This was clear through the noticeable increase in the mean of each of the peaks which means that there was an increase in the measurable energy of each recorded event or a higher ADC count. It was also shown that there was less light leakage with the new wrapping as compared to the original wrapping, or in other words, greater internal reflection. The generally lower standard deviation demonstrates that not only was there an increase in light yield, but a more precise measuring of the energies of the light collected. These results of an increase in light yield were evident in both the ^{60}Co and ^{241}Am experiments. Though the ^{241}Am test produced a slightly better resolution, the real resolving power was made evident in the ^{60}Co test. The two very closely residing peaks of ^{60}Co were significantly more resolved in the test with the new ESR material.

This increased light yield and better resolution will enable future measurements for the detection of lower energy particles as this new material is incorporated into more sophisticated detector setups. It would be especially beneficial in the efforts to detect the weak interactions WIMPs would make with normal matter.

4.2 Future Research

Now that this material has been proven highly effective in increasing overall light yield in CsI(Tl) scintillators, the material will be used in more advanced experimentation. The next experiment will be in a multi-scintillator detector (3 x 3) with this wrapping in our lab here on campus. This setup will further explore the detection of low energy particles especially in cryogenic conditions. This is apart of the SuperCDMS (Super Cryogenic Dark Matter Search) which our lab is working on along with Stanford University. The findings of these pioneering experiments will also be used at SNOLAB at Sudbury mines in Canada. However, in the near future, the 3M™ ESR wrapping will be used for all the crystals in a ton-scale project at Los Alamos National Laboratory.

REFERENCES

[1] N. A. Bahcall, "Dark matter universe," *Proceedings of the National Academy of Sciences*, vol. 112, no. 40, pp. 12243–12245, 2015.

[2] J. D. Lewin and P. F. Smith, "Review of mathematics, numerical factors, and corrections for dark matter experiments based on elastic nuclear recoil," *Astropart. Phys.*, vol. 6, pp. 87–112, 1996.

[3] G. F. Knoll, *Radiation detection and measurement*. 1989.

[4] S.-G. C. . Plastics, "Csi(tl), csi(na) cesium iodide scintillation material,"

[5] U.S.NRC, "Basic health physics - 07 - solid scintillators,"

[6] S. M. Y. K. M. S. V.V. Nagarkar, T.K. Gupta and G. Entine, "Structured csi(tl) scintillators for x-ray imaging applications," p. 5.

[7] 3M™, "3m™ enhanced specular reflector (esr),"

[8] A. U. Limited, "Csi(na)- cesium iodide (sodium)," p. 1.

[9] J. B. Dent, B. Dutta, A. Jastram, D. Kim, A. Kubik, R. Mahapatra, S. Rajendran, H. Ramani, A. Thompson, and S. Verma, "Pathfinder for a high statistics search for missing energy in gamma cascades," *Physical Review D*, vol. 105, jan 2022.

[10] S. A. Payne, S. Hunter, L. Ahle, N. J. Cherepy, and E. Swanberg, "Nonproportionality of scintillator detectors. iii. temperature dependence studies," *IEEE Transactions on Nuclear Science*, vol. 61, no. 5, pp. 2771–2777, 2014.